https://doi.org/10.5194/egusphere-2025-1595
Preprint. Discussion started: 15 May 2025

Hot spots, hot moments, and spatiotemporal drivers of soil CO_2 flux in temperate peatlands using UAV remote sensing

Yanfei Li[1]*, Maud Henrion[1], Angus Moore[1], Sébastien Lambot[1], Sophie Opfergelt[1], Veerle Vanacker[1], François Jonard[2†], Kristof Van Oost[1†]

[1] Earth and Life Institute, Université catholique de Louvain, 1348 Louvain-la-Neuve, Belgium.

[2] Earth Observation and Ecosystem Modelling Laboratory, SPHERES Research Unit, Université de Liège, 4000 Liège, Belgium.

**Correspondence to*: Yanfei Li (email: yanfei.li@uclouvain.be).

[†] These authors are co-last authors.

https://doi.org/10.5194/egusphere-2025-1595
Preprint. Discussion started: 15 May 2025

Abstract

CO_2 emissions from peatlands exhibit substantial spatial and temporal variability due to their heterogeneous nature, presenting challenges to identify their underlying drivers and to accurately quantify and model CO_2 fluxes. Here, we integrated field measurements with Unmanned Aerial Vehicle (UAV)-based multi-sensor remote sensing to investigate soil respiration across a temperate peatland landscape. Our research addressed two key questions: (1) How do environmental factors control the spatial-temporal distribution of soil respiration across complex landscapes? (2) How do hot spots and hot moments of biogeochemical processes influence landscape-level CO_2 fluxes? We find that dynamic variables (i.e., soil temperature and moisture) play significant roles in shaping CO_2 flux variations, contributing 43 % to seasonal variability and 29 % to spatial variance, followed by semi-dynamic variables (i.e., NDVI and root biomass) (19 % and 24 %). Relatively static variables (i.e., soil organic carbon (SOC) stock and C/N ratio) have a minimal influence on seasonal variation (2 %) but contribute more to spatial variance (10 %). Additionally, predicting time series of CO_2 fluxes is feasible by using key environmental variables (test set: $R^2 = 0.74$, $RMSE = 0.57$ µmol m^{-2} s^{-1}), while UAV remote sensing is an effective tool for mapping daily soil respiration (test set: $R^2 = 0.75$, $RMSE = 0.54$ µmol m^{-2} s^{-1}). By the integration of in-situ high-resolution time-lapse monitoring and spatial mapping, we find that despite occurring in 10 % of the year, hot moments contribute 28 %–31 % of the annual CO_2 fluxes. Meanwhile, hot spots—representing 10 % of the area—account for 20 % of CO_2 fluxes across the landscape. Our study demonstrates that integrating UAV-based remote sensing with field surveys improves the understanding of soil respiration mechanisms across timescales in complex landscapes, providing insights into carbon dynamics and supporting peatland conservation and climate change mitigation efforts.

Keywords: Peatlands, Soil respiration, Greenhouse gas (CO_2) emission, CO_2 hot spots, CO_2 hot moments, Multi-sensor UAV remote sensing, Global warming

https://doi.org/10.5194/egusphere-2025-1595
Preprint. Discussion started: 15 May 2025

1 Introduction

Peatlands are globally distributed ecosystems that store approximately 600 Gt of carbon (Yu et al., 2010), despite covering less than 4 % of the Earth's land surface (Xu et al., 2018). However, rising concerns exist over peatlands shifting from carbon sinks to carbon sources due to the impact of climate change (Dorrepaal et al., 2009; Huang et al., 2021; Hopple et al., 2020), land use/cover conversion (Leifeld et al., 2019; Deshmukh et al., 2021; Prananto et al., 2020), and other disturbances (Wilkinson et al., 2023; Turetsky et al., 2015). In Europe, it has been reported that nearly half of the peatlands are suffering degradation, primarily due to drainage for agricultural or forestry activities (Leifeld et al., 2019; Unep, 2022). As a consequence, European peatlands currently emit up to 580 Mt CO_2-eq per year across the continent (Unep, 2022). Given the critical role of the peatland ecosystem in the terrestrial carbon cycle, it is therefore important to understand the mechanisms driving carbon fluxes and their responses to climate change and human disturbances.

Soil respiration in peatlands is influenced by a combination of biotic and abiotic factors, such as soil temperature and moisture (Treat et al., 2014; Fang and Moncrieff, 2001; Juszczak et al., 2013; Swails et al., 2022; Hoyt et al., 2019; Evans et al., 2021), vegetation and root biomass (Acosta et al., 2017; Wang et al., 2021), and soil organic matter quality (Hoyos-Santillan et al., 2016; Leifeld et al., 2012). CO_2 emissions from peatlands are highly variable over space and time, presenting challenges to accurately quantify and model carbon fluxes. This may partial because peatlands are characterized by a unique microtopography, including features such as soil benches and depressions (Moore et al., 2019). These small-scale variations create differences in hydrology, temperature, biogeochemistry, and vegetation (Harris and Baird, 2019), leading to substantial spatial differences in the factors that control CO_2 fluxes and the formation of hot spots with elevated CO_2 emissions (Kelly et al., 2021; Becker et al., 2008; Mcclain et al., 2003; Frei et al., 2012; Kim and Verma, 1992). For instance, the peat surface temperature differences within a 10 m x 10 m plot characterized by hummock and hollow features can be 20°C (Rhoswen et al., 2018). In addition, peatlands experience highly variable weather conditions, which can trigger periods of disproportionately high CO_2 fluxes—often referred to as 'hot moments'—in response to transient environmental changes, such as sudden shifts in temperature, rainfall events, or fluctuations in the water table (Anthony and Silver, 2023). High CO_2 emissions occur from discrete areas in space (hot spots) and over short periods (hot moments), and may disproportionately contribute to the overall

https://doi.org/10.5194/egusphere-2025-1595
Preprint. Discussion started: 15 May 2025

fluxes (Anthony and Silver, 2023; Fernandez-Bou et al., 2020). Most studies have examined the mechanisms and contributions of hot spots and hot moments of other greenhouse gases (N_2O, CH_4) in agricultural and forestry ecosystems (Krichels and Yang, 2019; Anthony and Silver, 2021; Kannenberg et al., 2020; Leon et al., 2014; Fernandez-Bou et al., 2020), while research on CO_2 emission hot spots and hot moments in peatlands remains limited (Anthony and Silver, 2021, 2023).

Identifying and quantifying hot spots and hot moments in peatlands is challenging, requiring large-scale, continuous, long-term observations. Currently, most studies on peatland soil respiration rely on point measurements taken at intervals of half a month to one month, primarily during daytime (e.g., Wright et al. (2013); Bubier et al. (2003); Kim and Verma (1992); Danevčič et al. (2010)). This spatial-temporal limitation hinders the effective detection of hot spots and hot moments. Some studies attempted to extrapolate point data using land-use maps (Van Giersbergen et al., 2024; Webster et al., 2008; Mcnamara et al., 2008), but uncertainties in landscape-scale fluxes increase as the number of measurement locations decreases (Arias-Navarro et al., 2017; Wangari et al., 2022; Wangari et al., 2023). While automated chamber systems improve temporal resolution and help capture hot moments (Hoyt et al., 2019; Anthony and Silver, 2023), they are typically limited to a few sampling points, and scaling up is constrained by significant resource demands. Eddy covariance towers measure net ecosystem exchange over large areas by recording high-frequency CO_2 concentrations and air turbulence, providing insights into temporal variations at the ecosystem level (Rey-Sanchez et al., 2022; Abdalla et al., 2014). However, the underlying controlling factors and mechanisms at the process level are difficult to infer due to the large spatial footprint. In addition, they may not accurately represent the spatial heterogeneity of peatlands (Lees et al., 2018). These limitations highlight the need for complementary approaches to estimate CO_2 fluxes at the landscape scale with methods adapted for heterogeneous peatland ecosystems.

Several studies have integrated satellite-based remote sensing datasets with on-site chamber measurements to model landscape-scale CO_2 fluxes (e.g., Junttila et al. (2021); Wangari et al. (2023); Lees et al. (2018); Azevedo et al. (2021)). Remote sensing datasets on topography and vegetation parameters serve as proxies for soil moisture, vegetation cover, and nutrient availability, enabling large-scale CO_2 emission estimates within peatlands (Lees et al., 2018). However, this approach is somewhat limited by coarse spatial (10 m to 1 km) and temporal (1 to 16 days) resolutions, which may overlook

https://doi.org/10.5194/egusphere-2025-1595
Preprint. Discussion started: 15 May 2025

hot spots and hot moments, leading to potential over- or underestimations of CO_2 fluxes in heterogeneous peatlands (Kelly et al., 2021; Simpson, 2023). This shortcoming might be overcome by using unmanned aerial vehicles (UAVs) equipped with different kinds of sensors such as Red-Green-Blue (RGB), multispectral, thermal infrared, and Light Detection and Ranging (LiDAR). UAVs offer flexible deployment and capture high-resolution spatiotemporal data (1 cm to 1 m, minutes to months) (Minasny et al., 2019) which makes them particularly suitable for monitoring complex peatland dynamics and detecting hot spots and hot moments. Thus far, UAVs have proven to be reliable tools for peatland applications, including vegetation mapping (Steenvoorden et al., 2023), topographic reconstruction (Harris and Baird, 2019), peat depth and carbon storage estimation (Li et al., 2024), and moisture monitoring (Henrion et al., 2025). In a recent study, Kelly et al. (2021) utilized UAV-derived land surface temperature to estimate ecosystem respiration of a hemi-boreal fen in southern Sweden, and Pajula and Purre (2021) and Walcker et al. (2025) employed UAV-based multispectral vegetation indices to map ecosystem CO_2 flux at high resolution. These recent studies demonstrated the great potential of UAVs for linking CO_2 fluxes with environmental factors at a very high resolution, although they mainly focused on data from a single sensor. Few studies have explored the fusion of UAV-derived data from multiple sensors for mapping soil respiration across peatland landscapes.

In this study, we integrate multi-sensor UAV-based remote sensing with traditional field surveys to investigate soil respiration across a temperate peatland landscape, located in the Belgian Hautes Fagnes. As one of the largest and most ancient peatlands in Western Europe, the Belgian Hautes Fagnes represents an important ecosystem for studying peatland carbon fluxes due to its sensitivity to climate change and hydrological dynamics. Our research addresses two key questions: (1) What controls the nature and strength of the relationship between soil respiration and environmental factors across complex peatland landscapes and across spatial-temporal scales? (2) How do hot spots or hot moments of biogeochemical processes influence landscape-level carbon fluxes? More specifically, our study has three main objectives. First, we aim to identify the factors driving seasonal and spatial variations in soil respiration. Second, we assess the potential for linking environmental factors to CO_2 flux at high spatial and temporal resolutions. Third, we discuss the timing and location of hotspots and hot moments, assessing their contributions to overall CO_2 flux budgets.

https://doi.org/10.5194/egusphere-2025-1595
Preprint. Discussion started: 15 May 2025

2 Materials and methods

2.1 Study site

The Belgian Hautes Fagnes plateau, part of the Stavelot-Venn Massif, is located in eastern Belgium (Figure 1a). This elevated landscape experiences a humid climate, with mean annual air temperature and precipitation being approximately 6.7 °C and 1439.4 mm (period: 1971-2000), respectively (Mormal and Tricot, 2004). The peatlands in this region cover an area of 37.50 km^2, which primarily consist of raised bogs formed since the Late Pleistocene (Frankard et al., 1998). Our study site (50.49 N, 6.05 E; ~0.30 km^2) is located in the upper valley of the Hoëgne River peatland region (Figure 1a). The site is characterized by a distinct SE-NW oriented topographic gradient, with a clear transition from a low-relief plateau to steep hillslopes and then to the floodplain of a broad river valley (Sougnez and Vanacker, 2011). The area was drained and planted with spruces in 1914 and 1918. The plantations were progressively cleared between 2000 and 2016; since 2017, the site has been restored through reforestation with native hardwood species such as *Betula pubescens* and *Quercus robur*. Figure 1b shows main vegetation types across this landscape. An observation station of the Royal Meteorological Institute of Belgium (Mont Rigi, 50.51 N, 6.07 E) situated 3.07 km from the study site, records rainfall data every 10 minutes.

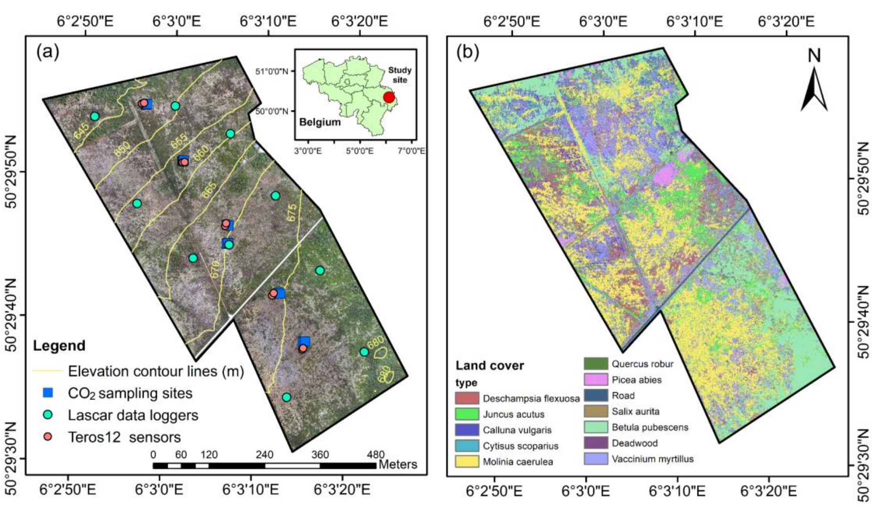

Figure 1. Maps showing the field-sampling locations (a) and land cover types (b) in the study area. Details on the land cover map are provided in our previous work (Li et al., 2024).

https://doi.org/10.5194/egusphere-2025-1595
Preprint. Discussion started: 15 May 2025

2.2 CO_2 flux measurement campaigns

Soil surface CO_2 flux measurements were conducted at five slope positions along the middle part of the site (Figure 1a). A portable infrared gas analyzer with an automated closed dynamic chamber (LI-8100A system, LI-COR, United States) was used to monitor CO_2 fluxes at 33 sites biweekly from December 2022 to March 2024 (Figure S1). At each slope position, six collars (20 cm diameter) were installed randomly, spaced 1–5 meters apart, to capture small-scale spatial variability. While at the shoulder, considering the heterogeneous soil water conditions, six collars were installed in drier areas and another three in wetter areas. All vegetation within the collars was removed. During each campaign, monitoring was conducted between 9:00 and 16:00. At each site, the CO_2 flux (μmol m^{-2} s^{-1}) in the chamber was measured for 2.5 minutes per observation. Simultaneously, soil surface temperature (0–10 cm) and volumetric water content (VWC) during each CO_2 measurement were recorded using a T-handled type-E thermocouple sensor (8100-201, LI-COR, United States) and a portable five-rod, 0.06 m long frequency domain reflectometry (FDR) probe system (ML2x, Delta-T, United Kingdom), respectively. However, CO_2 measurements were not always possible due to technical issues and bad weather conditions, resulting in a total of 666 valid measurements. In addition, a pair of soil CO_2 forced diffusion probes (eosFD, EOSense, United States) were installed near LI-8100A collars from 24 April 2024 to 8 November 2024 (Figure S1). These probes, consisting of a soil node and a reference node, are based on a membrane-based steady-state approach and can measure CO_2 flux every 5 minutes (Risk et al., 2011). During this period, the probes continuously monitored CO_2 flux at different slope positions (Figure S1), resulting in a total of 39476 valid flux measurements.

2.3 Temperature and soil moisture monitoring

The temporal evolution of soil temperature and moisture along the middle part was monitored using Teros12 sensors (Meter Group, München, Germany), with two replicates per slope position, spaced 5 meters apart (Figure 1a) (Henrion et al., 2025). These sensors recorded data at a depth of 10 cm from 14 October 2022 to 28 October 2024, every 10 minutes. Between the two replicates of each slope position, a station positioned ~1.4 m above the ground recorded air temperature every ten minutes. Additionally, ten soil temperature data loggers (EL-USB-1-PRO, Lascar, United Kingdom) were installed primarily along two evenly spaced transects parallel to the main slope, at a depth of 10 cm (Figure 1a). These

https://doi.org/10.5194/egusphere-2025-1595
Preprint. Discussion started: 15 May 2025

loggers recorded soil temperatures at the same frequency as Teros12 sensors from 21 March 2023 to 8 November 2024.

2.4 Soil sampling and laboratory analysis

After completing all gas sampling campaigns, 33 disturbed soil samples (0-10 cm depth) were collected within LI8100A collars at the five slope positions between 30 July and 15 October 2024. An Emlid Reach RS 2 GPS device with centimeter-level precision was used to record the sampling site locations, using a PPK solution with the Belgian WALCORS network. The samples were stored in a refrigerator until laboratory analysis. A subset of the samples was oven-dried at 80 °C for 24 hours (Dettmann et al., 2021), then crushed and ground into a fine powder for soil organic carbon (SOC) and total nitrogen content (TN) analysis (928 Series, LEGO, United States). Roots and litter were removed using tweezers during the pre-processing procedure. We tested the presence of inorganic carbon of each sample by adding one drop of 10 % HCl but found that no inorganic carbon was present in the samples. A subset of fresh samples was used for root biomass analysis. The fresh soil samples were weighed and placed in a 1 mm sieve, then rinsed with water to collect the roots. The washed roots were dried in an oven at 80 °C for 48 hours and then weighed to calculate their dry biomass.

2.5 UAV data acquisition and imagery processing

During the CO_2 flux monitoring period, we conducted regular UAV flights across the study area to collect high-resolution spatial data (Figure S1). A DJI Matrice 300 RTK was equipped with four different sensors: (i) a Red-Green-Blue (RGB) camera (DJI Zenmuse P1 camera, 35 mm and 45 MP), (ii) a multispectral camera (MicaSense RedEdge-M camera with five discrete spectral bands: blue (475 nm), green (560 nm), red (668 nm), rededge (717 nm), and near-infrared (842 nm), along with a downwelling light sensor), (iii) a LiDAR scanner (DJI Zenmuse L1, integrated with a 20-MP camera with a 1-inch CMOS sensor) and (iv) a thermal infrared camera (TeAX, featuring FLIR Tau2 cores and ThermalCapture hardware). Similar flight patterns and altitudes were used for the UAV missions as in our previous work (Li et al., 2024). In total, one RGB and one LiDAR dataset collected on 7 June 2023, were used in this study and ten multispectral and ten thermal datasets collected between 13 April 2023 and 13 May 2024.

The raw multispectral images were processed in the Pix4D mapper software (Pix4D S.A., Lausanne,

https://doi.org/10.5194/egusphere-2025-1595
Preprint. Discussion started: 15 May 2025

Switzerland) to generate reflectance maps (resolution: 6 cm) of the five spectral bands of the study area. We calculated the Normalized Difference Vegetation Index (NDVI) across the 10 maps from the monitoring period (Table S1). The raw thermal infrared video streams were converted into RJPG images using ThermoViewer version 3.0.26 (TeAX, 2022). Subsequently, the thermal images were processed with the Pix4D mapper to generate land surface temperature (LST) maps (resolution: 12 cm), which were used for soil temperature mapping (Text S1, Figure S2, Table S2). The RGB photos were processed in DJI Terra V4.0.10 (DJI, 2023) to generate an orthomosaic image with a resolution of 1.26 cm. The raw LiDAR data was processed in DJI Terra to provide a Digital Terrain Model (DTM; .tif file) with a resolution of 15 cm, which was used for generating daily air temperature maps (Text S1) and terrain wetness index (TWI) (Text S2). The variables derived from the four types of images were summarized in Table S1.

2.6 Statistical analysis

All data analyses were conducted in RStudio (v4.1.2). All timestamps in this study were converted to Coordinated Universal Time (UTC) to ensure consistency across datasets. Group differences were assessed by the one-way analysis of variance (*ANOVA*) using the *stats package*. When *ANOVA* detected a significant effect ($p < 0.05$), Tukey's Honestly Significant Difference (*HSD*) post-hoc test was performed to determine which groups differed significantly from each other. Pearson correlation analysis was performed using the *corrplot package* (Murdoch and Chow, 1996). The linear mixed-effects models used to identify factors controlling spatial- temporal variations of CO_2 flux, as well as time series simulation and mapping are introduced below.

2.6.1 Models to explain spatial-temporal variations in CO_2 flux

We utilized linear mixed-effects models to assess the impacts of both static and dynamic environmental factors on the spatial and seasonal variability of CO_2 fluxes. This is because mixed models integrate both fixed and random effects, which provide a robust framework for analyzing data with non-independent structures (Pinheiro and Bates, 2000). The model was performed using the *lme4 package* (Bates et al., 2015), with the natural logarithm of CO_2 flux observations as a response. The CO_2 fluxes data are often characterized by extreme values and right-skewed distribution, and a lognormal assumption for CO_2

https://doi.org/10.5194/egusphere-2025-1595
Preprint. Discussion started: 15 May 2025

fluxes could better account for the influences of extreme values on the overall distribution (Wutzler et al., 2020). The mixed-effects models were defined as:

$$y_{ij} = \beta_0 + \beta_1 x_{ij} + \cdots + \beta_p x_{ij} + b_{0j} + b_{1j} z_{ij} + \cdots + \epsilon_{ij} \qquad (1)$$

Where:

- y_{ij} is the dependent variable (i.e., ln (CO_2 flux), unit: μmol m^{-2} s^{-1}) for observations i in group j.
- β_0, β_1,…, β_p are fixed-effect coefficients.
- x_{ij} is the fixed-effect variable (independent variable).
- b_{0j}, b_{1j},… are random-effect coefficients associated with group j, which account for variability across groups.
- z_{ij} is the random-effect variable.
- ϵ_{ij} is the residual error term.

The fixed-effect predictors were categorized into three groups:

- Static variables: SOC stock, and the ratio of SOC content to nitrogen content (C/N ratio).
- Semi-dynamic variables: root biomass and NDVI.
- Dynamic variables: soil temperature and soil moisture at 0–10 cm depth.

Estimates for NDVI were extracted from the maps by retrieving the value of the 33 CO_2 flux observation sites and the SOC stock values were extracted from the a local high resolution (0.15 m) SOC stock map (Li et al., 2024). The sites were included as random effects in the seasonal pattern model to account for repeated measurements at the same locations during the monitoring period, whereas slope positions were treated as random effects in the spatial pattern model. Independent variable coefficients, Intraclass Correlation Coefficient (*ICC*), coefficients of determination (*marginal R^2* and *conditional R^2*), Root Mean Square Error (*RMSE*), and Akaike Information Criterion (*AIC*) were extracted using the *modelsummary package* after running each model. The *ICC* quantifies the proportion of variance explained by a grouping (random) factor in multilevel data; values close to 1 indicate high similarity within groups, while values near 0 suggest that grouping conveys little to no information (Nakagawa et al., 2017; Shrout and Fleiss, 1979). The *marginal R^2*, represents the variance explained by fixed effects alone, and *conditional R^2* represents the variance explained by both fixed and random effects (Pinheiro and Bates, 2000). The

https://doi.org/10.5194/egusphere-2025-1595
Preprint. Discussion started: 15 May 2025

relative importance of each independent variable was obtained using the *glmm.hp* package. To assess multicollinearity in regression analysis, the *car package* was used to calculate the variance inflation factor (*VIF*) (Fox and Monette, 1992).

2.6.2 Modelling hourly CO_2 flux

The mixed-effects model was utilized to simulate the time series of CO_2 fluxes at different slope positions. Here, the slope position was included as random variable, and the natural logarithm of CO_2 flux (hourly) was set as a response. We utilized CO_2 fluxes data measured by both the LI8100A system and eosFD probes. Specifically, we randomly selected a number of 30 observations from the eosFD probes at each slope position to reduce data redundancy from high-frequency sampling. Afterwards, we applied weighting to adjust the remaining imbalance in data density between the high-frequency eosFD monitoring and low-frequency LI8100A measurements, ensuring both data sources contributed proportionally to the model. The independent variables included hourly soil temperature (10 cm depth), volumetric soil moisture (VWC, 10 cm depth), and air temperature (1.4 m height), considering their importance in explaining the seasonal and diurnal patterns of CO_2 flux.

As in our previous work (Li et al., 2024), we divided the dataset into a training set (70 %) and a test set (30 %) using K-means clustering to minimize biases that could arise from random sampling (Hair et al., 2010). The models were trained on the training set, and the simulation accuracy was validated using the test dataset. The coefficient of determination (R^2) and *RMSE* were used to assess the quality of the model fit. Finally, we made simulations of the time series of hourly CO_2 flux for different slope positions from 1 May 2023 to 30 April 2024. Furthermore, we identified CO_2 emission hot moments based on the description in Section 2.6.4.

2.6.3 Mapping daily CO_2 flux

The linear mixed-effects model was utilized to map the spatial distribution of daily CO_2 fluxes across the landscape, with daily soil temperature (10 cm depth), corrected daily TWI, and SOC stock being considered as fixed-effect variables and gas sampling sites being included as random variables. The daily CO_2 flux model training, testing procedures, and evaluation of model fit followed the same approach detailed in Section 2.6.2. We then applied the trained model to predict the daily CO_2 flux of the landscape

https://doi.org/10.5194/egusphere-2025-1595
Preprint. Discussion started: 15 May 2025

from 1 May 2023 to 30 April 2024. Additionally, we calculated the mean daily soil CO_2 flux maps for each season and the entire year. Based on these predictions, we identified hot spots for each day by the methods described below.

2.6.4 Quantifying hot moments and hot spots of CO_2 flux

In previous studies, percentiles have been used as thresholds for identifying heat waves (e.g., (Meehl and Tebaldi, 2004): 97.5th percentile), soil heat extremes (e.g., García-García et al. (2023): 90th percentile), hot spots of N_2O emissions (e.g., Mason et al. (2017): median plus three times the interquartile range), and hot spots of CO_2 emissions (e.g., Wangari et al. (2023): median plus the interquartile range). In this study, we tested different methods and selected the 90th percentile as the threshold of both hot moments and hot spots to balance capturing extreme CO_2 emissions while maintaining a sufficient sample size. To capture the hot moments, we calculated a threshold for each slope position separately using its own dataset. For hot spots, we determined a daily threshold based on each map.

https://doi.org/10.5194/egusphere-2025-1595
Preprint. Discussion started: 15 May 2025

3 Results

3.1 Spatial and temporal patterns of CO_2 flux

During the monitoring period, the CO_2 emissions show large spatial and seasonal variations across the landscape. The CO_2 fluxes at the summit (3.16 ± 3.25 μmol m^{-2} s^{-1}) and shoulder (dry: 2.81 ± 3.22 μmol m^{-2} s^{-1}, wet: 2.33 ± 2.36 μmol m^{-2} s^{-1}) slope positions were significantly higher than that of footslope (1.25 ± 1.00 μmol m^{-2} s^{-1}) and backslope (1.11 ± 1.03 μmol m^{-2} s^{-1}) ($p < 0.05$) (Figure 2a). Furthermore, significant differences were observed when grouping the data into three vegetation covers: CO_2 emissions from *Vaccinium myrtillus* were lower than those from *Juncus acutus*, with mean ± sd values of 1.59 ± 1.43 μmol m^{-2} s^{-1}, and 2.33 ± 2.36 μmol m^{-2} s^{-1}, respectively (Figure 2b) ($p < 0.05$). However, the CO_2 fluxes under *Molinia caerulea* displayed large variations (0.02~20.1 μmol m^{-2} s^{-1}), and no significant differences were found compared to the other two vegetation types. The CO_2 flux data indicated large CO_2 emissions from June to September (3.65 ± 2.68 μmol m^{-2} s^{-1}), which can be 8.11 times higher than that from winter and early spring (0.45 ± 0.40 μmol m^{-2} s^{-1}) (Figure 2c). CO_2 emissions in May and October were at a moderate level.

https://doi.org/10.5194/egusphere-2025-1595
Preprint. Discussion started: 15 May 2025

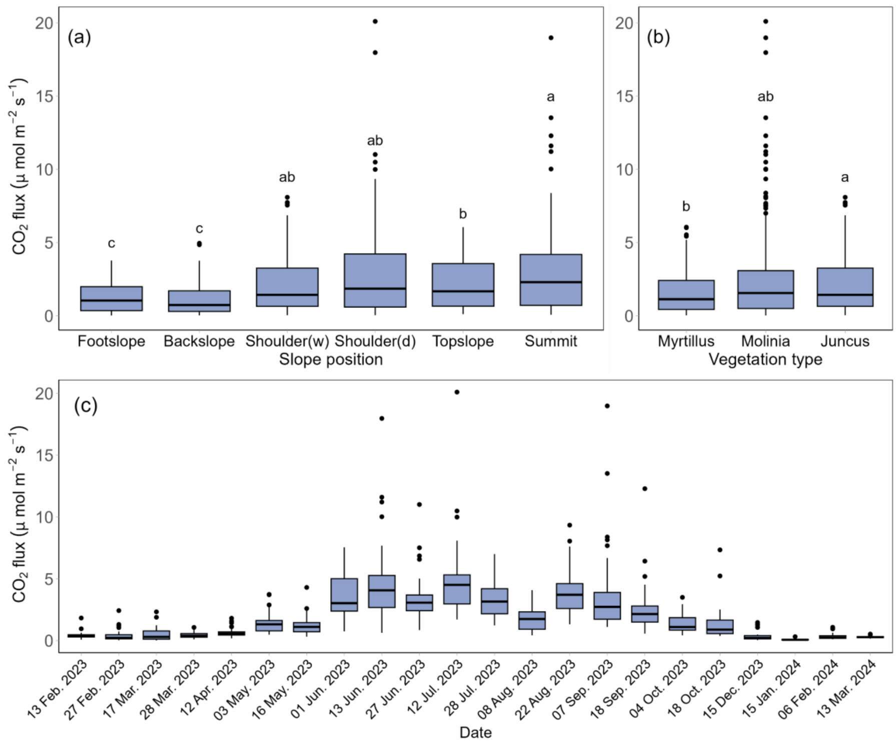

Figure 2. Boxplot of CO_2 flux (μmol m^{-2} s^{-1}) across different slope positions (a), vegetation types (b), and sampling dates (c), using data from the LI8100 A system recorded between 2023-02-13 and 2024-03-13. (a), CO_2 flux data of each box were from all dates, and Shoulder (w) and Shoulder (d) indicate shoulder wet and shoulder dry areas, respectively. (b), CO_2 flux data of each box were from all dates, and Myrtillus, Molinia and Juncus indicate *Vaccinium myrtillus*, *Molinia caerulea* and *Juncus acutus*, respectively. (c), CO_2 flux data of each box were from all slope positions. The edges of each box represent the first quartile (Q1) and third quartile (Q3), while the line inside the box indicates the median CO_2 flux. Whiskers extend from the box to the smallest and largest values within 1.5 times the interquartile range, and points outside the whiskers are considered extreme values. The *ANOVA* and *HSD* post-hoc tests were performed within slope positions and vegetation types, with boxes sharing the same letters indicating no significant difference.

3.2 Factors contributing to spatial-temporal variability

Three types of environmental factors explain 64 % of the observed seasonal variance in CO_2 emissions, with contributions of 33 % from soil temperature, 10 % from VWC, 19 % from vegetation (i.e., NDVI,

https://doi.org/10.5194/egusphere-2025-1595
Preprint. Discussion started: 15 May 2025

root biomass), 2 % from relatively static factors (i.e., SOC stock, C/N ratio), and 6 % from random effects (i.e., 33 sampling sites) (Table 1). This suggests that long-term stable environmental factors have minimal direct influence on seasonal CO_2 flux patterns. Interestingly, the contribution of these relatively stable factors is nearly 11 times higher in explaining overall spatial variations, although soil temperature is still the dominant factor (Table 1). The low *ICC* values in both spatial and seasonal models highlight significant small-scale heterogeneity in soil respiration.

Table 1. Coefficients and relative contributions of three types of input variables (static, semi-dynamic, dynamic) of mixed linear regression models for modelling CO_2 flux. Random effects were evaluated by *ICC* and model performance was evaluated by *Marginal R^2*, *Conditional R^2*, and *RMSE.*

	Input variables		Seasonal patterns	Spatial patterns
Fixed effects: coefficient (contribution)	Static	SOC stock ($t\ ha^{-1}$)	0.003 (1 %)	-0.003 (0.06 %)
		C/N ratio	0.05 (1 %)	0.07* (10 %)
	Semi dynamic	root biomass ($g\ 100g^{-1}$)	0.06 (0.36 %)	0.09* (12 %)
		NDVI	0.90*** (18 %)	-3.35** (12 %)
	Dynamic	Soil temp. (°C)	0.12*** (33 %)	0.39*** (18 %)
		VWC ($cm^3\ cm^{-3}$)	-0.77*** (10 %)	-1.37** (11 %)
Random effects	*ICC* (contribution)		0.18 (6 %)	0.06 (3 %)
Model performance	*Marginal R^2*		0.64	0.63
	Conditional R^2		0.70	0.66
	AIC		1386.00	50.10
	RMSE		0.64	0.25

Note. Significance level: *** $p < 0.001$, ** $p < 0.01$, * $p < 0.05$. All CO_2 fluxes (unit: μmol $m^{-2}\ s^{-1}$), soil temperature, and VWC data for spatial and seasonal patterns was from the LI8100 A system. To investigate the factors controlling spatial variations of CO_2 flux, we calculated the mean values of CO_2 flux, NDVI, soil temperature, and VWC of each site during the monitoring time.

https://doi.org/10.5194/egusphere-2025-1595
Preprint. Discussion started: 15 May 2025

3.3 Continuous hourly time series of CO_2 flux and hot moments

Three dynamic variables (i.e., soil temp., VWC, air temp.) were taken into account to predict the time series of hourly CO_2 flux at different slope positions. These input variables were selected due to their influential roles in explaining the diurnal (Figure S3) and seasonal fluctuations of CO_2 emissions. As shown in Table 2, the temporal model yielded a robust performance in both training and testing dataset, achieving R^2 and *RMSE* values of 0.86 and 0.39 μmol m^{-2} s^{-1} and 0.74 and 0.57 μmol m^{-2} s^{-1}, respectively.

Table 2. Model performance for simulating time series of hourly CO_2 flux (unit: μmol m^{-2} s^{-1}) and mapping daily CO_2 flux (unit: μmol m^{-2} s^{-1}) across the landscape.

Models	Training dataset		Testing dataset	
	RMSE	R^2	*RMSE*	R^2
Temporal model	0.39	0.86	0.57	0.74
Spatial model	0.50	0.81	0.54	0.75

Note. Temporal model used the natural logarithm of CO_2 flux data from LI8100 A and eosFD probes, whereas spatial model used the natural logarithm of CO_2 flux data only from LI8100 A.

The modelled CO_2 emissions at all slope positions display a clear seasonal trend, with higher CO_2 fluxes from June to September and lower estimates in other months, in line with the observed fluxes shown in brown dots (Figures 3c-3h). The total CO_2 fluxes (Table 3) at the summit (19.50 t ha^{-1}) and the shoulder (dry: 19.47 t ha^{-1}, wet: 16.31 t ha^{-1}) slope positions were higher than that of topslope (14.45 t ha^{-1}), followed by footslope (13.94 t ha^{-1}) and backslope (11.54 t ha^{-1}) (Table 3), consistent with the spatial patterns of our observations (Figure 3a). However, the modelled mean ± sd CO_2 fluxes at all slope positions (Table 3) were lower than measured CO_2 fluxes by the LI8100 A system. This is because the measurements were taken during the daytime when fluxes were higher (Figure 2), whereas the modeled values represent the average of both daytime and nighttime fluxes. Most hot moments occurred from June to September 2023, whereas few hot moments were observed from late July to the early August (Figures 3c-3h). Although these hot moments of different slope positions only accounted for 10 % across the year, they could contribute 28 %-31 % to the annual total CO_2 emissions (Table 3).

https://doi.org/10.5194/egusphere-2025-1595
Preprint. Discussion started: 15 May 2025

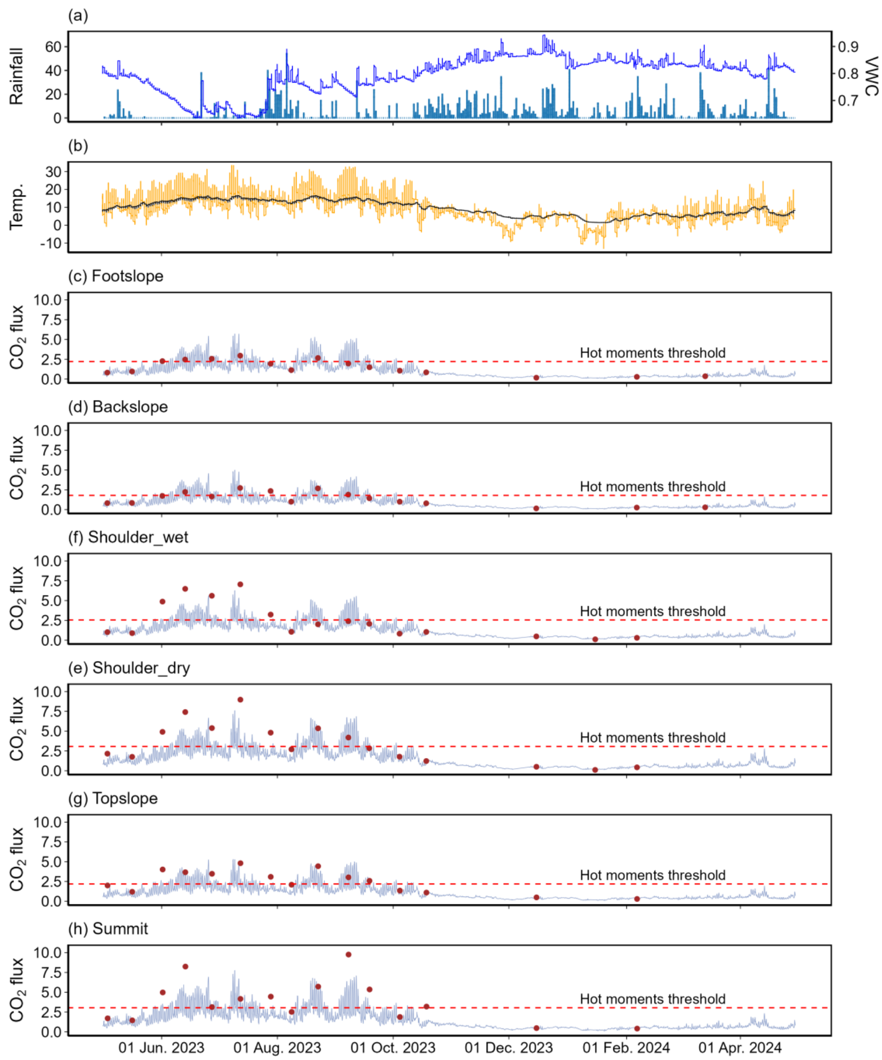

Figure 3. Time series of hourly rainfall (blue bar), hourly mean VWC (blue line) (a), hourly mean air temperature (orange line) and soil temperature (black line) (b), modelled hourly CO_2 flux (purple lines) and in-situ measurements (brown dots) at different slope positions (c-h). Rainfall (unit: mm) data was from the nearby meteorological observation station. The VWC (unit: cm^3 cm^{-3}) and soil temperature (unit: °C) were mean values from five slope positions monitored by Teros12 sensors at a depth of 10 cm. Air temperatures (unit: °C) were mean values from 5 stations at 1.4 m height above ground. Measured CO_2 fluxes (unit: µmol m^{-2} s^{-1}) were from the LI8100A system.

https://doi.org/10.5194/egusphere-2025-1595
Preprint. Discussion started: 15 May 2025

Table 3. Summary of modelled mean ± sd CO_2 fluxes, thresholds for identifying hot moments, total CO_2 flux, and the contribution of hot moments to total flux at different slope positions.

Slope position	Footslope	Backslope	Shoulder wet	Shoulder dry	Topslope	Summit
Mean ± sd CO_2 flux (μmol m^{-2} s^{-1})	1.00 ± 0.91	0.83 ± 0.73	1.21 ± 0.99	1.44 ± 1.22	1.04 ± 0.86	1.41 ± 1.22
Total CO_2 flux (t ha^{-1})	13.94	11.54	16.31	19.47	14.45	19.50
Threshold (μmol m^{-2} s^{-1})	2.22	1.80	2.55	3.07	2.19	3.04
Contribution of hot moments	30.74 %	30.31 %	28.99 %	28.41 %	28.91 %	29.93 %

3.4 Daily CO_2 flux maps and hot spots

A linear mixed-effects model was utilized to map daily CO_2 flux from 1 May 2023 to 30 April 2024, incorporating soil temperature, corrected TWI, and SOC stock as predictors due to their significant role in explaining the spatial-seasonal variability of CO_2 flux and their availability as spatial data. The mapping model yielded robust performance metrics (Table 2), with R^2 and *RMSE* values of 0.81 and 0.50 μmol m^{-2} s^{-1} in the training dataset, and 0.75 and 0.54 μmol m^{-2} s^{-1} in the test dataset, respectively.

Consistent with our observations, the modelled soil respiration also displayed substantial spatial-temporal heterogeneity (Figures 4a-4d). More specifically, the mean CO_2 fluxes ranged from 0.17 μmol m^{-2} s^{-1} to 10.80 μmol m^{-2} s^{-1} in spring (Figure 4a), 0.36 μmol m^{-2} s^{-1} to 30.60 μmol m^{-2} s^{-1} in summer (Figure 4b), 0.18 μmol m^{-2} s^{-1} to 14.87 μmol m^{-2} s^{-1} in autumn (Figure 4c), and 0.04 μmol m^{-2} s^{-1} to 2.24 μmol m^{-2} s^{-1} in winter (Figure 4d). Many modelled mean CO_2 fluxes at the footslope and backslope (elevation < 660 m) remained below 2 μmol m^{-2} s^{-1} (Figure 4e). In contrast, the modelled CO_2 emissions remained higher throughout the year at the shoulder (660 m ≤ elevation ≤ 670 m) and east of summit (elevation > 675 m) with high vegetation cover. About 10 % of the area were identified as hot spots, with a high frequency of hot spots occurring in these regions, while the locations of sporadic hot spots varied over time (Figure 4f). Overall, the landscape emitted approximately 24.34 t ha^{-1} CO_2 to the atmosphere during the simulation period, with 19.63 % ± 0.57 % of the CO_2 fluxes coming from the hot spots.

https://doi.org/10.5194/egusphere-2025-1595
Preprint. Discussion started: 15 May 2025

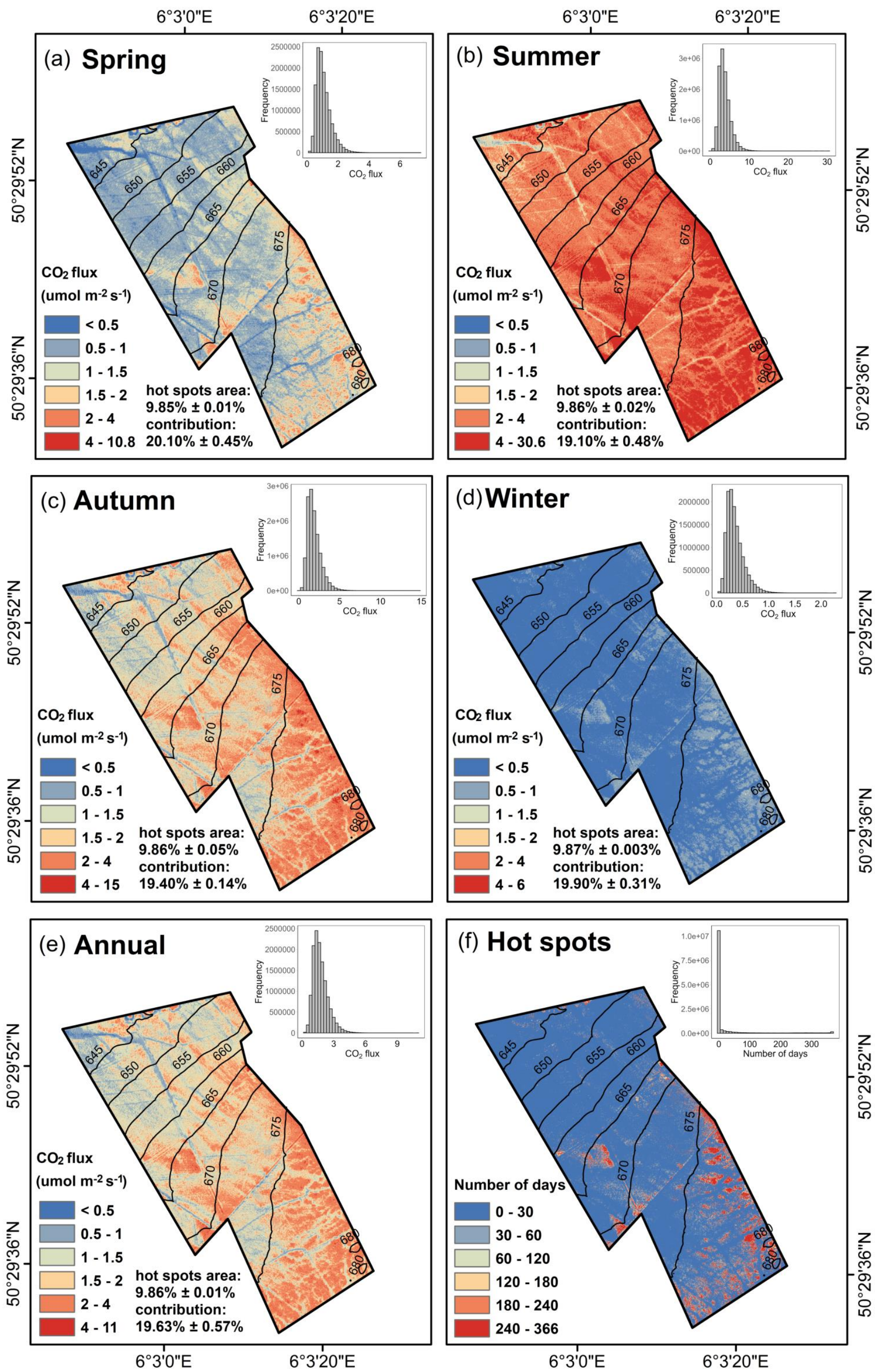

380

381 **Figure 4.** Maps of modelled mean daily CO_2 flux (μmol m^{-2} s^{-1}) in four seasons (a, b, c, d), throughout the year (e),

382 and hot spot frequency (f). The histograms of pixel values are presented on the top-right corner of each map. The

https://doi.org/10.5194/egusphere-2025-1595
Preprint. Discussion started: 15 May 2025

hot spots area proportion and CO_2 flux contribution from the hot spots of each season and across the year are summarized in the corresponding maps.

https://doi.org/10.5194/egusphere-2025-1595
Preprint. Discussion started: 15 May 2025

4 Discussion

4.1 Drivers of spatiotemporal heterogeneity in CO_2 emission

Consistent with prior temperate peatland studies (Juszczak et al., 2013; Wilson et al., 2015; Danevčič et al., 2010; Swails et al., 2022), our results indicate that seasonal variations in soil CO_2 flux across the landscape are highly related to soil temperature, which could account for 33 % of the seasonal variability (Table 1). In contrast to tropical peatlands, where precipitation or water table fluctuations often dominate CO_2 flux dynamics (Hoyt et al., 2019; Cobb et al., 2017), our observations reveal that temperature exhibits distinct seasonal patterns (Figure 3b), which in turn drive fluctuations in soil respiration throughout the year (Figure 2c). Moreover, spatial heterogeneity in soil temperature further shaped landscape-scale CO_2 emission patterns (Table 1). For instance, the south-facing summit slopes, which receive more solar radiation in the daytime, consistently show higher CO_2 fluxes (Figure 2a). Conversely, the north-facing footslope and backslope, situated on the windward side, experience lower temperatures, resulting in generally lower soil respiration rates throughout the observation period (Figure 2a). While temperature is the dominant driver, soil water content influences oxygen availability within the peat profile, thereby regulating microbial decomposition and CO_2 production (Hatala et al., 2012; Knox et al., 2015; Zou et al., 2022; Huang et al., 2021; Deshmukh et al., 2021). For example, Knox et al. (2015) demonstrated that a declining water table caused by drainage increases oxygen penetration into the peat, resulting in higher CO_2 flux compared to restored peatlands. In our study case, the CO_2 fluxes were slightly higher in drier shoulder positions compared to wetter areas (Figure 2a), and VWC accounted for approximately 10 % of the spatial-seasonal variance in CO_2 fluxes (Table 1).

The monthly/biweekly NDVI is the second-most influential predictor for CO_2 seasonal fluctuations (Table 1), as NDVI reveals vegetation phenology during the monitoring period. In the spatial-pattern model, the contribution from root biomass becomes more substantial, together with mean NDVI explaining 24 % of spatial variance. These findings align with previous studies that vegetation mediates soil respiration through root respiration, exudates, litter inputs, and rhizosphere priming effects (Acosta et al., 2017; Wang et al., 2015a; Walker et al., 2016; Jovani-Sancho et al., 2021; Bragazza et al., 2013). In our study, the CO_2 fluxes of dwarf shrubs (i.e., *Vaccinium myrtillus*) were significantly lower than those in *Juncus acutus*-dominated areas (Figure 2b), likely due to the lower root biomass of dwarf shrubs

https://doi.org/10.5194/egusphere-2025-1595
Preprint. Discussion started: 15 May 2025

(Table S3). Furthermore, it has been shown that dwarf shrubs in northern peatlands produce high-phenolic litter with higher resistance to breakdown and introduce more water-soluble phenolics into the soil compared to *Sphagnum*/herbs (Bragazza et al., 2013; Wang et al., 2015a), which further constrains microbial activity and CO_2 production. In addition, vegetation cover may indirectly influence soil respiration by regulating surface microclimate conditions such as humidity and temperature (Nichols, 1998; Stoy et al., 2012).

As shown in Table 1, the SOC stock and C/N ratio have limited explanatory power for the seasonal variability of CO_2 flux, in line with findings of Danevčič et al. (2010). However, when analyzing drivers of average soil CO_2 flux rate across the entire monitoring period, the importance of C/N ratio increased nearly 11 times (Table 1). This likely reflects how long-term averaging integrates short-term dynamic variability, thereby amplifying the role of spatial heterogeneity mediated by the C/N ratio. Prior studies suggesting that the quality of organic material, rather than its quantity, primarily regulates CO_2 fluxes in peatlands (Hoyos-Santillan et al., 2016; Leifeld et al., 2012). Specifically, the soil C/N ratio is known to regulate microbial community functionality and respiration intensity (Leifeld et al., 2020; Briones et al., 2014; Ishikura et al., 2018; Wang et al., 2015b).

4.2 CO_2 emission hot moments and hot spots: identification, implications, and importance

4.2.1 Temporal analysis and hot moments

During past decades, efforts have been made to model CO_2 flux over time based on its relationship with environmental factors such as hydrology, temperature, substrate quality, microbial community, and vegetation (Hoyt et al., 2019; Junttila et al., 2021; Schubert et al., 2010; Rowson et al., 2012; Abdalla et al., 2014; Farmer et al., 2011; Anthony and Silver, 2021). In our study, diurnal cycles of CO_2 fluxes are closely related to air temperature (Figure S3), while soil temperature and moisture are important factors in explaining the seasonal patterns of CO_2 flux (Table 1). Hence, the three dynamic environment variables were incorporated into the model to simulate the hourly CO_2 flux across the entire monitoring period. Overall, the temporal model demonstrated robust performance in both the training and testing datasets (Table 2) and effectively captured seasonal and diurnal trends at most sites (Figures 3c-3h). However, the modelled peak values are lower than the observations at shoulder and summit slope positions (Figures

https://doi.org/10.5194/egusphere-2025-1595
Preprint. Discussion started: 15 May 2025

3f, 3e, 3h), which may be partially due to the limited number of high-value observations in these areas. Consequently, the model is more influenced by the more frequent lower CO_2 fluxes, leading to an overall underestimation of the peak. In addition, two types of gas analyzers were employed to monitor CO_2 flux with different sampling frequency and time: the LI-8100A sensor was used biweekly or monthly to capture seasonal trends, while eosFD probes collected data every five minutes to track diurnal fluctuations. The integration of these datasets for modelling temporal dynamics improved estimation accuracy but might also introduce uncertainties into the model.

Anthony and Silver (2023) demonstrated that identifying hot moments of CO_2 flux in peatland requires intensive continuous measurements, while as an alternative, our robust simulation of hourly CO_2 flux enabled the identification of hot moments in a complex landscape. We found that most of these hot moments occurred during the summer and early autumn seasons (Figure 3c-3h), in agreement with our in-situ observations (Figure 2c). The frequent high CO_2 emissions in June and July can be attributed to the low precipitation, decreased soil moisture, and high temperatures (Figure 3a-3b). However, few hot moments were captured during late July and early August due to the heavy rainfall events (Figure 3a). This absence may be attributed to the fact that intense rainfall led to lower temperatures and increased soil moisture (Figures 3a, 3b), thereby suppressing microbial and root respiration (Hoyt et al., 2019). Following this period, CO_2 emissions reached values that exceeded the 'hot moments' threshold in mid-August, aligning with declining rainfall and rising temperatures (Figures 3c-3h). The hot moments observed in September are linked to seasonal fluctuations in precipitation and temperature (Figures 3a,3b).

Similar to the findings of Anthony and Silver (2021) and Kannenberg et al. (2020), these hot moments accounted for approximately 10 % throughout the year, while they contributed significantly to the annual total CO_2 emissions (28 %-31 %; Table 3), highlighting the important role of short-term high-emission events in the overall carbon emission. Therefore, missing hot moments may lead to significant underestimates of total peat soil respiration budgets. Despite continuous automated chamber or eddy covariance measurements that are ideal for capturing hot moments of CO_2 emissions (Anthony and Silver, 2023; Hoyt et al., 2019; Anthony and Silver, 2021), long-term continuous monitoring is still labor-intensive and cost-prohibitive in many locations within the complex peatland ecosystems. Given that we

https://doi.org/10.5194/egusphere-2025-1595
Preprint. Discussion started: 15 May 2025

observed a concentration of hot moments in the summer and autumn, we recommend increasing monitoring frequency during these seasons for temperate peatlands. This strategy would help capture carbon emission dynamics more effectively, reduce uncertainties in annual carbon flux estimates, and provide more representative peatland CO_2 flux data.

4.2.2 Spatial analysis of CO_2 fluxes and hot spots

Our mapping of CO_2 flux across the landscape yielded a model performance of $R^2 = 0.75$ and $RMSE$ = 0.54 μmol m^{-2} s^{-1} for the test dataset (Table 2). This can be attributed to the incorporation of key environmental factors that drive the spatiotemporal heterogeneity of soil respiration into the model inputs. These factors – including soil temperature, corrected TWI, and SOC stock – can be directly obtained through multi-sensor UAV remote sensing or estimated using high spatiotemporal resolution data. Previous studies upscaled spatial carbon fluxes using area-weighted methods, extrapolating point data from CO_2 chamber flux measurements to adjacent or larger areas based on land cover maps (Van Giersbergen et al., 2024; Webster et al., 2008; Leon et al., 2014). However, this approach can lead to over- or underestimation (Wangari et al., 2023; Leifeld and Menichetti, 2018), because our findings reveal that even within the same vegetation cover, such as *Molinia caerulea*, CO_2 emissions exhibit significant spatial-temporal variability (Figure 2b). In recent years, spatial upscaling of CO_2 fluxes has increasingly relied on satellite-based remote sensing data (e.g., Junttila et al. (2021); Wangari et al. (2023); Zhang et al. (2020); Azevedo et al. (2021); Huang et al. (2015). While this method covers larger areas, it is often constrained by coarse temporal and spatial resolutions. The peatland ecosystem is characterized by great temporal and spatial heterogeneity at small scales, and ignoring these variations can introduce significant uncertainties in CO_2 emission estimates. Our study demonstrates that high-resolution UAV remote sensing imagery, with fine temporal and spatial scales, could effectively upscale CO_2 fluxes from point measurements across a heterogeneous landscape, thereby reducing uncertainties in spatial predictions of CO_2 fluxes.

Furthermore, the high-resolution CO_2 flux maps allowed for the identification of hot spot areas across the landscape. We found that most of the hot spots occurred at the shoulder areas where soil moisture was relatively lower and to the east of the summit which is covered by dense vegetation (Figure 1b, Figure 4f). Spatial variability in the factors controlling biogeochemical processes, such as soil

https://doi.org/10.5194/egusphere-2025-1595
Preprint. Discussion started: 15 May 2025

temperature, moisture, water table depth, vegetation type, and substrate quality, is likely driving these differences (Anthony and Silver, 2023; Kuzyakov and Blagodatskaya, 2015; Mcnamara et al., 2008). For instance, the tree-covered areas at the summit contribute substantial root respiration, which may, in turn, trigger the formation of consistent hot pots throughout the year. Besides, litterfall beneath trees insulates the peat soil and provides an abundant resource for microbial activity.

High-emission events from hot spots play a crucial role in overall CO_2 fluxes (Anthony and Silver, 2023), hence, neglecting these areas could lead to substantial underestimation of peatland carbon emissions. In our study, although less than 10 % of area was identified as hot spots, their CO_2 flux contribution accounted for nearly 20 % across the year (Figure 4). However, research specifically focusing on peatland CO_2 emission hot spots remains limited (Anthony and Silver, 2023), despite increased exploration of greenhouse gas emission hot spots in other ecosystems (e.g., agricultural field (Krichels and Yang, 2019; Rey-Sanchez et al., 2022; Leifeld et al., 2020); wetland (Rey-Sanchez et al., 2022); water-limited Mediterranean ecosystem (Leon et al., 2014); forest (Wangari et al., 2023)). Hence, to improve the accuracy of CO_2 spatial budgeting for peatlands, there is a need for enhanced high-resolution dynamic monitoring of hot spot areas (Becker et al., 2008). Our study demonstrates the great potential of UAV technology for peatland hot spot identification and quantification, offering new insights into studying soil respiration within heterogeneous ecosystems as well as optimizing peatland management and CO_2 emission reduction strategies.

https://doi.org/10.5194/egusphere-2025-1595
Preprint. Discussion started: 15 May 2025

5 Conclusion

In this study, we monitored the dynamics of peatland surface and subsurface environments using both field surveys and multi-sensor UAVs at high spatial-temporal resolution. We investigated the influence of dynamic and static environmental factors on soil respiration rates across different scales, thereby enhancing our understanding of peatland carbon cycling. Additionally, we simulated CO_2 flux with high spatial-temporal resolution by integrating field measurements and UAV data. These reliable modelling allow us to identify and quantify CO_2 emission hot spots and hot moments across the landscape. To summarize, the main findings of our study are as follows:

(1) Soil respiration rates vary significantly across space and time, influenced by both dynamic and relatively static environmental factors at different scales. Temperature is the primary driver of CO_2 flux variations, explaining 33 % CO_2 seasonal variability and 18 % spatial variability. Soil moisture negatively affects both seasonal and spatial variations, accounting for 10 % - 11 % of the variance. Semi-dynamic factors (i.e., NDVI and root biomass) contribute 19 % to seasonal variability and 24 % to spatial variability. While relative static factors (i.e., the C/N and SOC stock) have little impact on the seasonal CO_2 flux variability, the contribution of the C/N ratio increases nearly 11 times for spatial variability.

(2) Predicting temporal series of hourly CO_2 flux can be effectively achieved (test set: $R^2 = 0.74$, $RMSE = 0.57$ μmol m^{-2} s^{-1}) by considering its relationship with key environmental variables such as air temperature, soil temperature and soil moisture, all of which are relatively straightforward to monitor. These reliable time series data provide a foundation for capturing respiration pulses occurring over short periods, with hot moments primarily occurring in summer and early autumn.

(3) The UAV remote sensing data can yield robust spatial mapping of soil respiration rates across heterogeneous landscapes, with *RMSE* and R^2 values of 0.54 μmol m^{-2} s^{-1} and 0.75 in the test dataset, respectively. These high-resolution CO_2 flux maps enable us to locate hot spots.

(4) Despite representing 10 % of time within one year, CO_2 fluxes from hot moments contribute 28 %-31 % to the overall CO_2 flux budgets. Approximately 10 % areas are identified as hot spots, while contributing 19.63 % ± 0.57 % of total CO_2 fluxes. The locations of high-frequency hot spots remain consistent, while the locations of sporadic hot spots vary over time.

https://doi.org/10.5194/egusphere-2025-1595
Preprint. Discussion started: 15 May 2025

Code and data availability

Code and data will be made available on request.

CRediT authorship contribution statement

YL: Writing – original draft, Visualization, Investigation, Formal analysis, Conceptualization. **MH**: Writing – review & editing, Investigation. **AM**: Writing – review & editing. **SL**: Writing – review & editing, Funding acquisition, Conceptualization. **SO**: Writing – review & editing, Funding acquisition, Conceptualization. **VV**: Writing – review & editing, Funding acquisition, Conceptualization. **FJ**: Writing – review & editing, Funding acquisition, Supervision, Conceptualization. **KVO**: Writing – review & editing, Investigation, Funding acquisition, Supervision, Conceptualization.

Declaration of Competing Interest

The authors declare that they do not have any commercial or associative interest that represents a conflict of interest in connection with the work submitted.

Acknowledgements

Yanfei Li wishes to thank the joint grant from China Scholarship Council and UCLouvain (No. 202106380030). Kristof Van Oost, Sophie Opfergelt, and Sébastien Lambot are supported by the *Fonds de la Recherche Scientifique* (FNRS). The authors would like to thank the *Département de la Nature et des Forêts* (DNF) and Joël Verdin for giving access to the study site. The authors would like to thank Dylan Vellut for his assistance with soil respiration measurements and UAV campaigns.

Financial support

This work is an *Action de Recherche Concertée*, n° 21/26–119, funded by the *Communauté française de Belgique*.

https://doi.org/10.5194/egusphere-2025-1595
Preprint. Discussion started: 15 May 2025

References

Abdalla, M., Hastings, A., Bell, M. J., Smith, J. U., Richards, M., Nilsson, M. B., Peichl, M., Löfvenius, M. O., Lund, M., Helfter, C., Nemitz, E., Sutton, M. A., Aurela, M., Lohila, A., Laurila, T., Dolman, A. J., Belelli-Marchesini, L., Pogson, M., Jones, E., Drewer, J., Drosler, M., and Smith, P.: Simulation of CO2 and Attribution Analysis at Six European Peatland Sites Using the ECOSSE Model, Water, Air, & Soil Pollution, 225, 2182, 10.1007/s11270-014-2182-8, 2014.

Acosta, M., Juszczak, R., Chojnicki, B., Pavelka, M., Havránková, K., Lesny, J., Krupková, L., Urbaniak, M., Machačová, K., and Olejnik, J.: CO2 Fluxes from Different Vegetation Communities on a Peatland Ecosystem, Wetlands, 37, 423-435, 10.1007/s13157-017-0878-4, 2017.

Anthony, T. L. and Silver, W. L.: Hot moments drive extreme nitrous oxide and methane emissions from agricultural peatlands, Global Change Biology, 27, 5141-5153, https://doi.org/10.1111/gcb.15802, 2021.

Anthony, T. L. and Silver, W. L.: Hot spots and hot moments of greenhouse gas emissions in agricultural peatlands, Biogeochemistry, 10.1007/s10533-023-01095-y, 2023.

Arias-Navarro, C., Díaz-Pinés, E., Klatt, S., Brandt, P., Rufino, M. C., Butterbach-Bahl, K., and Verchot, L. V.: Spatial variability of soil N2O and CO2 fluxes in different topographic positions in a tropical montane forest in Kenya, Journal of Geophysical Research: Biogeosciences, 122, 514-527, https://doi.org/10.1002/2016JG003667, 2017.

Azevedo, O., Parker, T. C., Siewert, M. B., and Subke, J.-A.: Predicting Soil Respiration from Plant Productivity (NDVI) in a Sub-Arctic Tundra Ecosystem, 10.3390/rs13132571, 2021.

Bates, D., Mächler, M., Bolker, B., and Walker, S.: Fitting Linear Mixed-Effects Models Using lme4, Journal of Statistical Software, 67, 1 - 48, 10.18637/jss.v067.i01, 2015.

Becker, T., Kutzbach, L., Forbrich, I., Schneider, J., Jager, D., Thees, B., and Wilmking, M.: Do we miss the hot spots? – The use of very high resolution aerial photographs to quantify carbon fluxes in peatlands, Biogeosciences, 5, 1387-1393, 10.5194/bg-5-1387-2008, 2008.

Bragazza, L., Parisod, J., Buttler, A., and Bardgett, R. D.: Biogeochemical plant–soil microbe feedback in response to climate warming in peatlands, Nature Climate Change, 3, 273-277, 10.1038/nclimate1781, 2013.

Briones, M. J. I., McNamara, N. P., Poskitt, J., Crow, S. E., and Ostle, N. J.: Interactive biotic and abiotic regulators of soil carbon cycling: evidence from controlled climate experiments on peatland and boreal

https://doi.org/10.5194/egusphere-2025-1595
Preprint. Discussion started: 15 May 2025

soils, Global Change Biology, 20, 2971-2982, https://doi.org/10.1111/gcb.12585, 2014.

Bubier, J. L., Bhatia, G., Moore, T. R., Roulet, N. T., and Lafleur, P. M.: Spatial and Temporal Variability in Growing-Season Net Ecosystem Carbon Dioxide Exchange at a Large Peatland in Ontario, Canada, Ecosystems, 6, 353-367, 10.1007/s10021-003-0125-0, 2003.

Cobb, A. R., Hoyt, A. M., Gandois, L., Eri, J., Dommain, R., Abu Salim, K., Kai, F. M., Haji Su'ut, N. S., and Harvey, C. F.: How temporal patterns in rainfall determine the geomorphology and carbon fluxes of tropical peatlands, Proceedings of the National Academy of Sciences, 114, E5187-E5196, 10.1073/pnas.1701090114, 2017.

Danevčič, T., Mandic-Mulec, I., Stres, B., Stopar, D., and Hacin, J.: Emissions of CO2, CH4 and N2O from Southern European peatlands, Soil Biology and Biochemistry, 42, 1437-1446, https://doi.org/10.1016/j.soilbio.2010.05.004, 2010.

Deshmukh, C. S., Julius, D., Desai, A. R., Asyhari, A., Page, S. E., Nardi, N., Susanto, A. P., Nurholis, N., Hendrizal, M., Kurnianto, S., Suardiwerianto, Y., Salam, Y. W., Agus, F., Astiani, D., Sabiham, S., Gauci, V., and Evans, C. D.: Conservation slows down emission increase from a tropical peatland in Indonesia, Nature Geoscience, 14, 484-490, 10.1038/s41561-021-00785-2, 2021.

Dorrepaal, E., Toet, S., van Logtestijn, R. S. P., Swart, E., van de Weg, M. J., Callaghan, T. V., and Aerts, R.: Carbon respiration from subsurface peat accelerated by climate warming in the subarctic, Nature, 460, 616-619, https://doi.org/10.1038/nature08216, 2009.

Evans, C. D., Peacock, M., Baird, A. J., Artz, R. R. E., Burden, A., Callaghan, N., Chapman, P. J., Cooper, H. M., Coyle, M., Craig, E., Cumming, A., Dixon, S., Gauci, V., Grayson, R. P., Helfter, C., Heppell, C. M., Holden, J., Jones, D. L., Kaduk, J., Levy, P., Matthews, R., McNamara, N. P., Misselbrook, T., Oakley, S., Page, S. E., Rayment, M., Ridley, L. M., Stanley, K. M., Williamson, J. L., Worrall, F., and Morrison, R.: Overriding water table control on managed peatland greenhouse gas emissions, Nature, 593, 548-552, 10.1038/s41586-021-03523-1, 2021.

Fang, C. and Moncrieff, J. B.: The dependence of soil CO2 efflux on temperature, Soil Biology and Biochemistry, 33, 155-165, https://doi.org/10.1016/S0038-0717(00)00125-5, 2001.

Farmer, J., Matthews, R., Smith, J. U., Smith, P., and Singh, B. K.: Assessing existing peatland models for their applicability for modelling greenhouse gas emissions from tropical peat soils, Current Opinion in Environmental Sustainability, 3, 339-349, https://doi.org/10.1016/j.cosust.2011.08.010, 2011.

https://doi.org/10.5194/egusphere-2025-1595
Preprint. Discussion started: 15 May 2025

Fernandez-Bou, A. S., Dierick, D., Allen, M. F., and Harmon, T. C.: Precipitation-drainage cycles lead to hot moments in soil carbon dioxide dynamics in a Neotropical wet forest, Global Change Biology, 26, 5303-5319, 10.1111/gcb.15194, 2020.

Fox, J. and Monette, G.: Generalized Collinearity Diagnostics, Journal of the American Statistical Association, 87, 178-183, https://doi.org/10.2307/2290467, 1992.

Frankard, P., Ghiette, P., Hindryckx, M.-N., Schumacker, R., and Wastiaux, C.: Peatlands of Wallony (S-Belgium), SUO, Helsinki, Finland, 01/01, 33-37,

Frei, S., Knorr, K. H., Peiffer, S., and Fleckenstein, J. H.: Surface micro-topography causes hot spots of biogeochemical activity in wetland systems: A virtual modeling experiment, Journal of Geophysical Research: Biogeosciences, 117, https://doi.org/10.1029/2012JG002012, 2012.

García-García, A., Cuesta-Valero, F. J., Miralles, D. G., Mahecha, M. D., Quaas, J., Reichstein, M., Zscheischler, J., and Peng, J.: Soil heat extremes can outpace air temperature extremes, Nature Climate Change, 13, 1237-1241, 10.1038/s41558-023-01812-3, 2023.

Harris, A. and Baird, A. J.: Microtopographic Drivers of Vegetation Patterning in Blanket Peatlands Recovering from Erosion, Ecosystems, 22, 1035-1054, https://doi.org/10.1007/s10021-018-0321-6, 2019.

Hatala, J. A., Detto, M., Sonnentag, O., Deverel, S. J., Verfaillie, J., and Baldocchi, D. D.: Greenhouse gas (CO2, CH4, H2O) fluxes from drained and flooded agricultural peatlands in the Sacramento-San Joaquin Delta, Agriculture, Ecosystems & Environment, 150, 1-18, https://doi.org/10.1016/j.agee.2012.01.009, 2012.

Henrion, M., Li, Y., Wu, K., Jonard, F., Opfergelt, S., Vanacker, V., Van Oost, K., and Lambot, S.: Drone-Borne Ground-Penetrating Radar Reveals Spatiotemporal Moisture Dynamics in Peatland Root Zones, Available at SSRN, http://dx.doi.org/10.2139/ssrn.5098978, 2025.

Hopple, A. M., Wilson, R. M., Kolton, M., Zalman, C. A., Chanton, J. P., Kostka, J., Hanson, P. J., Keller, J. K., and Bridgham, S. D.: Massive peatland carbon banks vulnerable to rising temperatures, Nature Communications, 11, 2373, 10.1038/s41467-020-16311-8, 2020.

Hoyos-Santillan, J., Lomax, B. H., Large, D., Turner, B. L., Boom, A., Lopez, O. R., and Sjögersten, S.: Quality not quantity: Organic matter composition controls of CO2 and CH4 fluxes in neotropical peat profiles, Soil Biology and Biochemistry, 103, 86-96, https://doi.org/10.1016/j.soilbio.2016.08.017, 2016.

https://doi.org/10.5194/egusphere-2025-1595
Preprint. Discussion started: 15 May 2025

Hoyt, A. M., Gandois, L., Eri, J., Kai, F. M., Harvey, C. F., and Cobb, A. R.: CO2 emissions from an undrained tropical peatland: Interacting influences of temperature, shading and water table depth, Global Change Biology, 25, 2885-2899, https://doi.org/10.1111/gcb.14702, 2019.

Huang, N., Gu, L., Black, T. A., Wang, L., and Niu, Z.: Remote sensing-based estimation of annual soil respiration at two contrasting forest sites, Journal of Geophysical Research: Biogeosciences, 120, 2306-2325, https://doi.org/10.1002/2015JG003060, 2015.

Huang, Y., Ciais, P., Luo, Y., Zhu, D., Wang, Y., Qiu, C., Goll, D. S., Guenet, B., Makowski, D., De Graaf, I., Leifeld, J., Kwon, M. J., Hu, J., and Qu, L.: Tradeoff of CO2 and CH4 emissions from global peatlands under water-table drawdown, Nature Climate Change, 11, 618-622, https://doi.org/10.1038/s41558-021-01059-w, 2021.

Ishikura, K., Darung, U., Inoue, T., and Hatano, R.: Variation in Soil Properties Regulate Greenhouse Gas Fluxes and Global Warming Potential in Three Land Use Types on Tropical Peat, 10.3390/atmos9120465, 2018.

Jovani-Sancho, A. J., Cummins, T., and Byrne, K. A.: Soil carbon balance of afforested peatlands in the maritime temperate climatic zone, Global Change Biology, 27, 3681-3698, https://doi.org/10.1111/gcb.15654, 2021.

Junttila, S., Kelly, J., Kljun, N., Aurela, M., Klemedtsson, L., Lohila, A., Nilsson, M. B., Rinne, J., Tuittila, E.-S., Vestin, P., Weslien, P., and Eklundh, L.: Upscaling Northern Peatland CO2 Fluxes Using Satellite Remote Sensing Data, 10.3390/rs13040818, 2021.

Juszczak, R., Humphreys, E., Acosta, M., Michalak-Galczewska, M., Kayzer, D., and Olejnik, J.: Ecosystem respiration in a heterogeneous temperate peatland and its sensitivity to peat temperature and water table depth, Plant and Soil, 366, 505-520, 10.1007/s11104-012-1441-y, 2013.

Kannenberg, S. A., Bowling, D. R., and Anderegg, W. R. L.: Hot moments in ecosystem fluxes: High GPP anomalies exert outsized influence on the carbon cycle and are differentially driven by moisture availability across biomes, Environmental Research Letters, 15, 054004, 10.1088/1748-9326/ab7b97, 2020.

Kelly, J., Kljun, N., Eklundh, L., Klemedtsson, L., Liljebladh, B., Olsson, P.-O., Weslien, P., and Xie, X.: Modelling and upscaling ecosystem respiration using thermal cameras and UAVs: Application to a peatland during and after a hot drought, Agricultural and Forest Meteorology, 300, 108330,

https://doi.org/10.5194/egusphere-2025-1595
Preprint. Discussion started: 15 May 2025

https://doi.org/10.1016/j.agrformet.2021.108330, 2021.

Kim, J. and Verma, S. B.: Soil surface CO2 flux in a Minnesota peatland, Biogeochemistry, 18, 37-51, 10.1007/BF00000425, 1992.

Knox, S. H., Sturtevant, C., Matthes, J. H., Koteen, L., Verfaillie, J., and Baldocchi, D.: Agricultural peatland restoration: effects of land-use change on greenhouse gas (CO2 and CH4) fluxes in the Sacramento-San Joaquin Delta, Global Change Biology, 21, 750-765, https://doi.org/10.1111/gcb.12745, 2015.

Krichels, A. H. and Yang, W. H.: Dynamic Controls on Field-Scale Soil Nitrous Oxide Hot Spots and Hot Moments Across a Microtopographic Gradient, Journal of Geophysical Research: Biogeosciences, 124, 3618-3634, https://doi.org/10.1029/2019JG005224, 2019.

Kuzyakov, Y. and Blagodatskaya, E.: Microbial hotspots and hot moments in soil: Concept & review, Soil Biology and Biochemistry, 83, 184-199, https://doi.org/10.1016/j.soilbio.2015.01.025, 2015.

Lees, K. J., Quaife, T., Artz, R. R. E., Khomik, M., and Clark, J. M.: Potential for using remote sensing to estimate carbon fluxes across northern peatlands – A review, Science of The Total Environment, 615, 857-874, https://doi.org/10.1016/j.scitotenv.2017.09.103, 2018.

Leifeld, J. and Menichetti, L.: The underappreciated potential of peatlands in global climate change mitigation strategies, Nature Communications, 9, 1071, 10.1038/s41467-018-03406-6, 2018.

Leifeld, J., Klein, K., and Wüst-Galley, C.: Soil organic matter stoichiometry as indicator for peatland degradation, Scientific Reports, 10, 7634, 10.1038/s41598-020-64275-y, 2020.

Leifeld, J., Steffens, M., and Galego-Sala, A.: Sensitivity of peatland carbon loss to organic matter quality, Geophysical Research Letters, 39, https://doi.org/10.1029/2012GL051856, 2012.

Leifeld, J., Wüst-Galley, C., and Page, S.: Intact and managed peatland soils as a source and sink of GHGs from 1850 to 2100, Nature Climate Change, 9, 945-947, 10.1038/s41558-019-0615-5, 2019.

Leon, E., Vargas, R., Bullock, S., Lopez, E., Panosso, A. R., and La Scala, N.: Hot spots, hot moments, and spatio-temporal controls on soil CO2 efflux in a water-limited ecosystem, Soil Biology and Biochemistry, 77, 12-21, https://doi.org/10.1016/j.soilbio.2014.05.029, 2014.

Li, Y., Henrion, M., Moore, A., Lambot, S., Opfergelt, S., Vanacker, V., Jonard, F., and Van Oost, K.: Factors controlling peat soil thickness and carbon storage in temperate peatlands based on UAV high-resolution remote sensing, Geoderma, 449, 117009, https://doi.org/10.1016/j.geoderma.2024.117009,

https://doi.org/10.5194/egusphere-2025-1595
Preprint. Discussion started: 15 May 2025

2024.

Mason, C. W., Stoof, C. R., Richards, B. K., Das, S., Goodale, C. L., and Steenhuis, T. S.: Hotspots of Nitrous Oxide Emission in Fertilized and Unfertilized Perennial Grasses, Soil Science Society of America Journal, 81, 450-458, https://doi.org/10.2136/sssaj2016.08.0249, 2017.

McClain, M. E., Boyer, E. W., Dent, C. L., Gergel, S. E., Grimm, N. B., Groffman, P. M., Hart, S. C., Harvey, J. W., Johnston, C. A., Mayorga, E., McDowell, W. H., and Pinay, G.: Biogeochemical Hot Spots and Hot Moments at the Interface of Terrestrial and Aquatic Ecosystems, Ecosystems, 6, 301-312, 10.1007/s10021-003-0161-9, 2003.

McNamara, N. P., Plant, T., Oakley, S., Ward, S., Wood, C., and Ostle, N.: Gully hotspot contribution to landscape methane (CH4) and carbon dioxide (CO2) fluxes in a northern peatland, Science of The Total Environment, 404, 354-360, https://doi.org/10.1016/j.scitotenv.2008.03.015, 2008.

Meehl, G. A. and Tebaldi, C.: More Intense, More Frequent, and Longer Lasting Heat Waves in the 21st Century, Science, 305, 994-997, 10.1126/science.1098704, 2004.

Minasny, B., Berglund, Ö., Connolly, J., Hedley, C., de Vries, F., Gimona, A., Kempen, B., Kidd, D., Lilja, H., Malone, B., McBratney, A., Roudier, P., O'Rourke, S., Rudiyanto, Padarian, J., Poggio, L., ten Caten, A., Thompson, D., Tuve, C., and Widyatmanti, W.: Digital mapping of peatlands – A critical review, Earth-Science Reviews, 196, 102870, https://doi.org/10.1016/j.earscirev.2019.05.014, 2019.

Moore, P. A., Lukenbach, M. C., Thompson, D. K., Kettridge, N., Granath, G., and Waddington, J. M.: Assessing the peatland hummock–hollow classification framework using high-resolution elevation models: implications for appropriate complexity ecosystem modeling, Biogeosciences, 16, 3491-3506, 10.5194/bg-16-3491-2019, 2019.

Mormal, P. and Tricot, C.: Aperçu climatique des Hautes-Fagnes, Institut Royal météorologique de Belgique, Brussel, 2004.

Murdoch, D. J. and Chow, E. D.: A Graphical Display of Large Correlation Matrices, The American Statistician, 50, 178-180, https://doi.org/10.2307/2684435, 1996.

Nakagawa, S., Johnson, P. C. D., and Schielzeth, H.: The coefficient of determination R2 and intra-class correlation coefficient from generalized linear mixed-effects models revisited and expanded, Journal of The Royal Society Interface, 14, 20170213, 10.1098/rsif.2017.0213, 2017.

Nichols, D. S.: Temperature of upland and peatland soils in a north central Minnesota forest, Canadian

https://doi.org/10.5194/egusphere-2025-1595
Preprint. Discussion started: 15 May 2025

Journal of Soil Science, 78, 493-509, 10.4141/S96-030, 1998.

Pajula, R. and Purre, A.-H.: NDVI as a proxy to estimate the CO2 fluxes in peatlands: example of alkaline fen, The 16th International Peatland Congress: Peatland and Peat - Source of Ecosystem Services, Tallinn, Estonia,

Pinheiro, J. C. and Bates, D. M.: Fitting Linear Mixed-Effects Models, in: Mixed-Effects Models in S and S-PLUS, edited by: Pinheiro, J. C., and Bates, D. M., Springer New York, New York, NY, 133-199, 10.1007/0-387-22747-4_4, 2000.

Prananto, J. A., Minasny, B., Comeau, L.-P., Rudiyanto, R., and Grace, P.: Drainage increases CO2 and N2O emissions from tropical peat soils, Global Change Biology, 26, 4583-4600, https://doi.org/10.1111/gcb.15147, 2020.

Rey-Sanchez, C., Arias-Ortiz, A., Kasak, K., Chu, H., Szutu, D., Verfaillie, J., and Baldocchi, D.: Detecting Hot Spots of Methane Flux Using Footprint-Weighted Flux Maps, Journal of geophysical research. Biogeosciences, 127, e2022JG006977, 10.1029/2022jg006977, 2022.

Rhoswen, L., Rhoswen, L., Nicholas, K., Nicholas, K., Devito, K. J., Kevin, J. D., Kevin, D., Richard, M. P., Richard, M. P., Carl, M., Carl, A. M., Waddington, J. M., James, M. W., Stefan, K., and Stefan, K.: Disturbance Impacts on Thermal Hot Spots and Hot Moments at the Peatland-Atmosphere Interface, Geophysical Research Letters, 10.1002/2017gl075974, 2018.

Risk, D., Nickerson, N., Creelman, C., McArthur, G., and Owens, J.: Forced Diffusion soil flux: A new technique for continuous monitoring of soil gas efflux, Agricultural and Forest Meteorology, 151, 1622-1631, https://doi.org/10.1016/j.agrformet.2011.06.020, 2011.

Rowson, J., Worrall, F., Evans, M., and Dixon, S.: Predicting soil respiration from peatlands, Science of The Total Environment, 442C, 397-404, 10.1016/j.scitotenv.2012.10.021, 2012.

Schubert, P., Eklundh, L., Lund, M., and Nilsson, M.: Estimating northern peatland CO2 exchange from MODIS time series data, Remote Sensing of Environment, 114, 1178-1189, https://doi.org/10.1016/j.rse.2010.01.005, 2010.

Shrout, P. E. and Fleiss, J. L.: Intraclass correlations: Uses in assessing rater reliability, Psychological Bulletin, 86, 420-428, 10.1037/0033-2909.86.2.420, 1979.

Simpson, G.: Drivers of peatland CO_2 balance: a fusion of UAV remote sensing and micrometeorology, Doctoral dissertation, School of GeoSciences, The University of Edinburgh, U.K., 57-157 pp.,

https://doi.org/10.5194/egusphere-2025-1595
Preprint. Discussion started: 15 May 2025

http://dx.doi.org/10.7488/era/3228, 2023.

Sougnez, N. and Vanacker, V.: The topographic signature of Quaternary tectonic uplift in the Ardennes massif (Western Europe), Hydrol. Earth Syst. Sci., 15, 1095-1107, https://doi.org/10.5194/hess-15-1095-2011, 2011.

Steenvoorden, J., Bartholomeus, H., and Limpens, J.: Less is more: Optimizing vegetation mapping in peatlands using unmanned aerial vehicles (UAVs), International Journal of Applied Earth Observation and Geoinformation, 117, 103220, https://doi.org/10.1016/j.jag.2023.103220, 2023.

Stoy, P. C., Street, L. E., Johnson, A. V., Prieto-Blanco, A., and Ewing, S. A.: Temperature, Heat Flux, and Reflectance of Common Subarctic Mosses and Lichens under Field Conditions: Might Changes to Community Composition Impact Climate-Relevant Surface Fluxes?, Arctic, Antarctic, and Alpine Research, 44, 500-508, 10.1657/1938-4246-44.4.500, 2012.

Swails, E. E., Ardón, M., Krauss, K. W., Peralta, A. L., Emanuel, R. E., Helton, A. M., Morse, J. L., Gutenberg, L., Cormier, N., Shoch, D., Settlemyer, S., Soderholm, E., Boutin, B. P., Peoples, C., and Ward, S.: Response of soil respiration to changes in soil temperature and water table level in drained and restored peatlands of the southeastern United States, Carbon Balance and Management, 17, 18, 10.1186/s13021-022-00219-5, 2022.

Treat, C. C., Wollheim, W. M., Varner, R. K., Grandy, A. S., Talbot, J., and Frolking, S.: Temperature and peat type control CO2 and CH4 production in Alaskan permafrost peats, Global Change Biology, 20, 2674-2686, 10.1111/gcb.12572, 2014.

Turetsky, M. R., Benscoter, B., Page, S., Rein, G., van der Werf, G. R., and Watts, A.: Global vulnerability of peatlands to fire and carbon loss, Nature Geoscience, 8, 11-14, 10.1038/ngeo2325, 2015.

UNEP: Global Peatlands Assessment – The State of the World's Peatlands: Evidence for action toward the conservation, restoration, and sustainable management of peatlands, Global Peatlands Initiative, United Nations Environment Programme9789280739916, 125-154, https://doi.org/10.59117/20.500.11822/41222, 2022.

van Giersbergen, Q., Barthelmes, A., Couwenberg, j., Fritz, C., Lång, K., Martin, N., and Tanneberger, F.: Identifying hotspots of greenhouse gas emissions from drained peatlands in the European Union, PREPRINT (Version 1) available at Research Square, https://doi.org/10.21203/rs.3.rs-4629642/v1, 2024.

Walcker, R., Le Lay, C., Gandois, L., Elger, A., and Jassey, V. E. J.: High-resolution mapping of peatland

https://doi.org/10.5194/egusphere-2025-1595
Preprint. Discussion started: 15 May 2025

CO2 fluxes using drone multispectral images, Ecological Informatics, 103060, https://doi.org/10.1016/j.ecoinf.2025.103060, 2025.

Walker, T. N., Garnett, M. H., Ward, S. E., Oakley, S., Bardgett, R. D., and Ostle, N. J.: Vascular plants promote ancient peatland carbon loss with climate warming, Global Change Biology, 22, 1880-1889, https://doi.org/10.1111/gcb.13213, 2016.

Wang, H., Richardson, C. J., and Ho, M.: Dual controls on carbon loss during drought in peatlands, Nature Climate Change, 5, 584-587, 10.1038/NCLIMATE2643, 2015a.

Wang, H., Tian, J., Chen, H., Ho, M., Vilgalys, R., Bu, Z.-J., Liu, X., and Richardson, C. J.: Vegetation and microbes interact to preserve carbon in many wooded peatlands, Communications Earth & Environment, 2, 67, 10.1038/s43247-021-00136-4, 2021.

Wang, M., Moore, T. R., Talbot, J., and Riley, J. L.: The stoichiometry of carbon and nutrients in peat formation, Global Biogeochemical Cycles, 29, 113-121, https://doi.org/10.1002/2014GB005000, 2015b.

Wangari, E. G., Mwangada Mwanake, R., Houska, T., Kraus, D., Gettel, G. M., Kiese, R., Breuer, L., and Butterbach-Bahl, K.: Identifying landscape hot and cold spots of soil greenhouse gas fluxes by combining field measurements and remote sensing data, Biogeosciences, 20, 5029-5067, 10.5194/bg-20-5029-2023, 2023.

Wangari, E. G., Mwanake, R. M., Kraus, D., Werner, C., Gettel, G. M., Kiese, R., Breuer, L., Butterbach-Bahl, K., and Houska, T.: Number of Chamber Measurement Locations for Accurate Quantification of Landscape-Scale Greenhouse Gas Fluxes: Importance of Land Use, Seasonality, and Greenhouse Gas Type, Journal of Geophysical Research: Biogeosciences, 127, e2022JG006901, https://doi.org/10.1029/2022JG006901, 2022.

Webster, K. L., Creed, I. F., Beall, F. D., and Bourbonnière, R. A.: Sensitivity of catchment-aggregated estimates of soil carbon dioxide efflux to topography under different climatic conditions, Journal of Geophysical Research: Biogeosciences, 113, https://doi.org/10.1029/2008JG000707, 2008.

Wilkinson, S. L., Andersen, R., Moore, P. A., Davidson, S. J., Granath, G., and Waddington, J. M.: Wildfire and degradation accelerate northern peatland carbon release, Nature Climate Change, 13, 456-461, https://doi.org/10.1038/s41558-023-01657-w, 2023.

Wilson, D., Dixon, S. D., Artz, R. R. E., Smith, T. E. L., Evans, C. D., Owen, H. J. F., Archer, E., and Renou-Wilson, F.: Derivation of greenhouse gas emission factors for peatlands managed for extraction

https://doi.org/10.5194/egusphere-2025-1595
Preprint. Discussion started: 15 May 2025

in the Republic of Ireland and the United Kingdom, Biogeosciences, 12, 5291-5308, 10.5194/bg-12-5291-2015, 2015.

Wright, E. L., Black, C. R., Turner, B. L., and Sjögersten, S.: Environmental controls of temporal and spatial variability in and fluxes in a neotropical peatland, Global Change Biology, 19, 3775-3789, https://doi.org/10.1111/gcb.12330, 2013.

Wutzler, T., Perez-Priego, O., Morris, K., El-Madany, T. S., and Migliavacca, M.: Soil CO2 efflux errors are lognormally distributed – implications and guidance, Geosci. Instrum. Method. Data Syst., 9, 239-254, 10.5194/gi-9-239-2020, 2020.

Xu, J., Morris, P. J., Liu, J., and Holden, J.: PEATMAP: Refining estimates of global peatland distribution based on a meta-analysis, CATENA, 160, 134-140, https://doi.org/10.1016/j.catena.2017.09.010, 2018.

Yu, Z., Loisel, J., Brosseau, D. P., Beilman, D. W., and Hunt, S. J.: Global peatland dynamics since the Last Glacial Maximum, Geophysical Research Letters, 37, https://doi.org/10.1029/2010GL043584, 2010.

Zhang, C., Comas, X., and Brodylo, D.: A Remote Sensing Technique to Upscale Methane Emission Flux in a Subtropical Peatland, Journal of Geophysical Research: Biogeosciences, 125, e2020JG006002, https://doi.org/10.1029/2020JG006002, 2020.

Zou, J., Ziegler, A. D., Chen, D., McNicol, G., Ciais, P., Jiang, X., Zheng, C., Wu, J., Wu, J., Lin, Z., He, X., Brown, L. E., Holden, J., Zhang, Z., Ramchunder, S. J., Chen, A., and Zeng, Z.: Rewetting global wetlands effectively reduces major greenhouse gas emissions, Nature Geoscience, 15, 627-632, 10.1038/s41561-022-00989-0, 2022.